ISSN 1516-392X

AUTOMATIC CLASSIFICATION OF INCLUSIONS IN STEEL[1]

Aline Christina Stein Cechin[2]
Sidnei Paciornik[3]

Resumo
An image analysis (IA) routine is proposed to automate the classification of inclusions in steels. Based on the charts from ASTM E-45, an algorithm discriminates types A, B, C, and D, after automatically building stringers aligned along the rolling direction (RD) for types B and C. Mathematical morphology operations were used to build the stringers from individual aligned inclusions. The method then proceeds to distinguish inclusions and/or stringers into the thin and thick series, according to the standard. For stringers, a specific routine was developed to measure the total length along RD for thin and thick inclusions, and automatically establishes the final stringer thickness. Finally, the severity is obtained through the measurement of the total length (or count) of inclusions and stringers for the thin and thick series. The method is successful for the figures presented in the standard charts. Initial results for real images indicate that the method compares well with manual measurements by an experimented operator, but with better sampling and much increased speed.
Key words: Steel; Inclusions; Image analysis; Digital microscopy.

CLASSIFICAÇÃO AUTOMÁTICA DE INCLUSÕES EM AÇO

Resumo
Materiais compósitos contém ao menos duas fases - uma matriz contínua e uma fase descontínua de reforço. Isto leva a um grande número de possíveis arranjos do reforço, que precisam ser caracterizados para permitir a previsão das propriedades do material.Os modelos matemáticos para compósitos exigem a determinação de diversos parâmetros microestruturais tais como fração volumétrica, distribuição de tamanho, orientação e espacial do reforço. No entanto, os métodos tradicionais de caracterização não oferecem a abrangência, velocidade e exatidão estatística requeridas. Parâmetros como distribuição de forma, espacial e orientacional não são facilmente obtidos. A Microscopia Digital (MD) é a convergência de automação do microscópio, aquisição, processamento e análise de imagens. No presente trabalho o impacto da MD na caracterização de materiais compósitos é apresentado. Novos métodos são discutidos e a microestrutura de compósitos de matriz polimérica reforçados por fibras ou partículas é descrita. Isto permite a determinação de parâmetros críticos usados no modelamento das propriedades dos materiais.
Palavras-chave: Aço; Inclusões; Análise de imagens; Microscopia digital.

[1] *Technical contribution to 65th ABM Annual Congress, July, 26th to 30h, 2010, Rio de Janeiro, RJ, Brazil.*
[2] *Undergraduate student – DEMa/PUC-Rio*
[3] *Electronic Engineer and Physicist, D.Sc, Associate Professor. – DEMa/PUC-Rio*

1 INTRODUCTION

The main goal of the present work is to develop an automatic method for the classification of inclusions in steels. Traditionally, two ASTM standards are used as reference to this kind of classification.
E-45 – "Standard Test Methods for Determining the Inclusion Content of Steels" [1] – establishes the procedures for manual classification, many times based in chart comparison, in which an operator observes an image field under the microscope, and compares it to the templates drawn in reference charts.
E-1122 – "Standard Practice for Obtaining JK Inclusion Ratings Using Automatic Image Analysis"[2] – establishes quantitative methods based on image analysis (IA) to identify and classify inclusions in images. In this case, one aims at making the procedure less operator dependent.
In both aforementioned cases inclusion classification is based in the following criteria:
Inclusion type – discriminating the inclusions in types A (sulfides), B (alumina), C (silicates), and D (oxides).
Stringer formation – stringers are groups of inclusions aligned in the rolling direction (RD) of the steel, with maximum intra-group spacing defined by the standard, and that must be treated as a single object. This definition is applicable to B and C type inclusions.
Thickness or diameter of inclusions or stringers – separating in the so-called thin and tick series, with different limits for each inclusion type.
Severity (S) – a measure of inclusion density in each measured area. This measure is obtained through the total length of inclusions, for type A, total length of stringers, for B and C types, or from a direct count, for D inclusions.
The two critical points, among the steps cited above, are the identification of inclusion types and stringer formation. E-1122 proposes to start by separating type A inclusions, which appear with lighter intensity than the other types. Then, to identify type C inclusions by their elongated shape, in contrast to the more equiaxial shapes of types B and D. Supposing these two steps are successful, it is necessary to group like inclusions that belong to any given stringer, so as to allow the classification in the thin and thick series and, finally, measure the total length that leads to the severity.
From these definitions, it becomes evident that the classification procedure can be strongly operator dependent, so that an automatic approach is welcome.

2 TRAINING BASED ON REFERENCE IMAGES

The first step in the development of the proposed method was to digitize the reference charts of the E-45 standard, which contains figures for the 4 inclusion types, thin and thick series and 6 severity levels (from 0.5 to 3.0 in 0.5 steps), adding up to 48 figures. From these digital images, image processing and analysis routines were developed to automate the classification. As the chart figures have accurate x-y calibration and also possess manual measurements of severity, they constitute an excellent reference for the calibration of automatic routines. Figure 1 shows a subset of the figures from the chart, depicting 4 inclusion types, thick series and severity 3.0.

ISSN 1516-392X

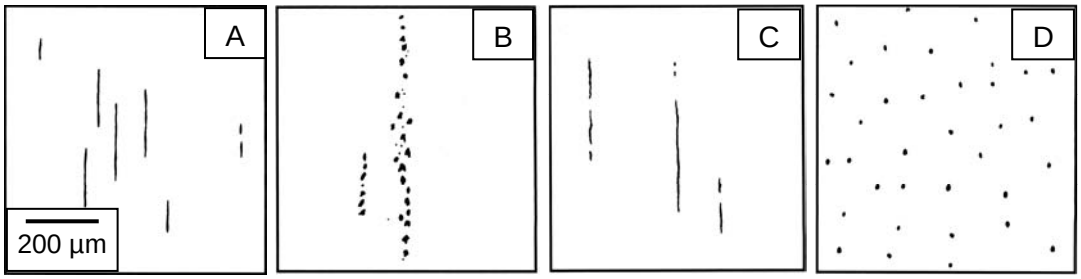

Figure 1 – Digitized images from the E-45 reference chart. Types A, B, C e D, thick series, S = 3.0.

2.1 Reference Images with Separated Types and Thicknesses

2.1.1. Stringer formation and severity measurements

The 48 figures were separately processed aiming at, initially, measuring the severity through image analysis and comparing with the values informed in the chart.

The analysis of type D images is trivial, since it implies in simply counting the number of objects. Analysis of type A is also relatively simple since the severity depends on the total length of inclusions in the field. However, the processing of types B and C is more demanding, since inclusions must first be assembled into stringer before the total length is measured to provide severity. The standard establishes rules for the concatenation of inclusions in a given stringer, such as the minimum number of inclusions and maximum distance between them. For type C, for example, two inclusions pertain to the same stringer if the distance between them along the rolling direction is <= 40 µm.

Thus, employing the KS400 software (Carl Zeiss Vision), a set of routines was developed to process the images, segment the inclusions, impose controlled and directional dilation along the RD to build stringers, when necessary, and obtain the total length. As examples, Table 1 shows the results obtained for type A (direct measurement of total length) and type C (requiring stringer formation first). These results are compared to the values quoted in the reference charts.

Table 1 – Comparison of severity measurements obtained by image analysis and from the standard reference charts

	Class A (values in µm)			Class C (values in µm)		
Severity	Reference length value	Measured length value – thin series	Measured length value – thick series	Reference length value	Measured length value – thin series	Measured length value – thick series
0.5	37.0	37.57	37.57	18.0	18.8	18.4
1.0	127.0	127.23	128.08	76.0	76.0	76.4
1.5	261.0	260.86	264.7	176.0	174.6	172.5
2.0	436.0	422.67	420.11	320.0	320.2	319.4
2.5	649.0	696.76	696.34	510.0	532.4	533.7
3.0	898.0	914.93	916.64	746.0	758.7	744.2

One can see that the values obtained through IA are accurate, with maximum relative error of 7.3% for type A and 4.6% for type C. These discrepancies may be due to small spatial calibration errors, distortions during scanning or even errors in the reference charts, since those measurements were obtained by traditional manual methods.

The measurement of the severity for type B is harder because the definition for stringer formation is more complex. In this case stringers are formed by at least 3 inclusions aligned along RD, and that must be less than 15 µm from the middle point of the formed stringer. Moreover, differently from type A and C inclusions, which are elongated along RD, type B inclusions are equiaxial and faceted objects. Thus, identifying their alignment axis is not evident, what requires some extra processing steps, listed in the following.

Determination of the x-y aligned convex hull[3] for all objects, thus creating an aligned rectangular boundary for each inclusion. Each rectangle is then filled and dilated with and horizontal structuring element (SE).[4] The aim of this step is to compensate a possible misalignment of inclusions along the RD, so that the inclusions can be identified as pertaining to a stringer, in the following step. The standard rule for inclusion concatenation into stringers is then applied. This is done through a morphological closing (dilation followed by erosion) with vertical SE and a number of steps obtained through the inclusion distance defined in the standard.

Figure 2 shows an example of the obtained result. In the final image inclusions are shown in red while stringers obtained through image processing are shown in white.

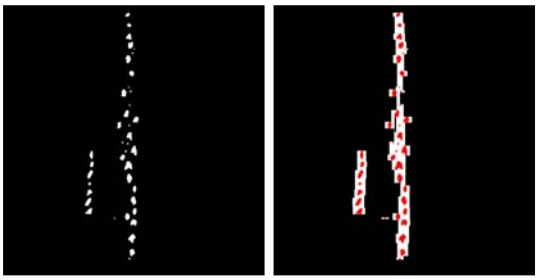

Figure 2 – Original and processed image for type B inclusions, thick series, severity 3.0.

Once stringers are formed their total length can be measured. Table 2 shows the obtained results compared to the values quoted in the reference charts. The largest relative error is 4%, attesting to the accuracy of the developed routine.

Table 2 – Severity measurements obtained through IA after stringer formation compared to reference values. Type B inclusions

	Class B (values in µm)		
Severity	Reference Value	Measured length value – thin series	Measured length value – thick series
0.5	17.0	16.65	17.08
1.0	77.0	74.71	73.86
1.5	184.0	184.01	187.43
2.0	343.0	353.08	336.00
2.5	555.0	563.56	565.27
3.0	822.0	828.26	837.23

2.2 Reference Images Containing Mixed Types and Thicknesses

The tests describe so far are a simplification since each images contains inclusions of a single type and thickness. With the aim of approaching a more realistic situation, the chart reference images were digitally combined. Figure 3 shows one such combination containing thin and thick inclusions of type B (S = 1, 2, 2.5), type C (S = 0.5, 1, 2, 2.5), and type D (S = 1).

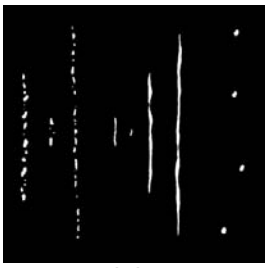

Figure 3 – Synthetic image containing types B, C, and D inclusions from fields of different severities and thicknesses.

2.2.1 Identification of inclusion type

An image processing routine was developed to distinguish inclusions by their types (A, B, C, D), based on shape variations between inclusions or stringers. The main steps are described in the following:

1. Separation of A type inclusions by their brightness. According to the standard this discrimination should be done based on the lighter tone of sulfides when compared to the other types. However, as the reference charts present black and white images, this separation was not done at this point. However, it is feasible in real samples.
2. To allow distinguishing B type from D Type inclusions and other low severity inclusions or stringers, all inclusions were dilated along the RD (Figure 4a). Then, using the length of dilated B inclusions with S = 2.0 as a threshold, shorter objects were eliminated, leaving behind dilated higher severity type B and long type C inclusions (Figure 4b). Intersecting the resulting image with the original recovers the original shape of the inclusions (Figure 4c). Then, using the length of type C S=1.0 as a threshold for object elimination, one is left behind with type B inclusions with S>=1.0 (Figure 4d).

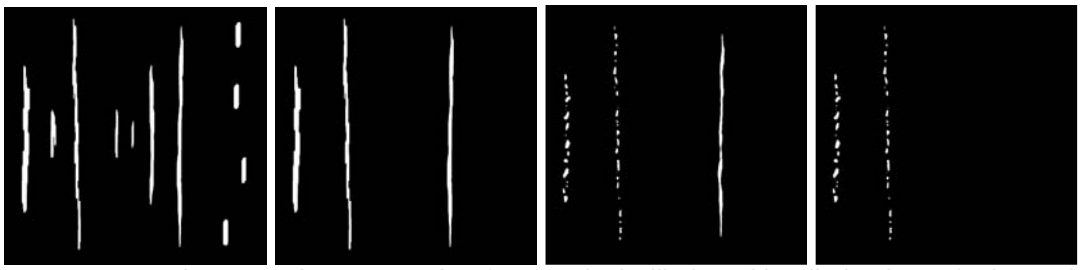

Figure 4 – Second processing step. a) After vertical dilation. b) Elimination of short objects. c) Intersection of the result in b with the original image. d) Type B S>=2.0.

3. Again using the length of type C S=1.0 inclusions as a threshold, all type C inclusions, except with S=0.5, were separated. See Figure 5.

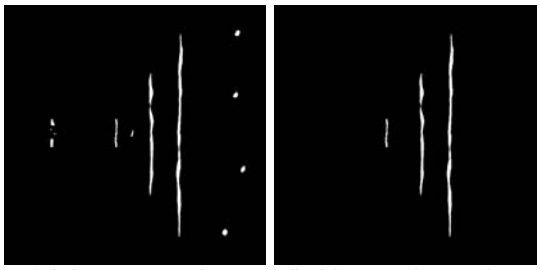

Figure 5 – a) Result of (Figure 3 – Figure 4d). b) Keeping only type C S>0.5.

4. With the aim of separating lower severity type B inclusions, the remaining objects from step 3 were obtained and dilated. A new length threshold was used, slightly shorter than dilated type B S=1.0 inclusions, eliminating all but type B S<2. The sequence is illustrated in Figure 6.

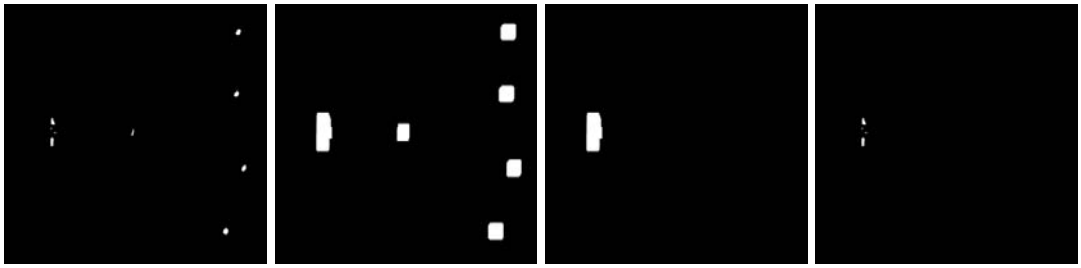

Figure 6 – a) Result of (Figure 5a – Figure 5b). b) After dilation. c) Dilated type B. d) Inclusions of type B S< 2.0.

5. The aspect ratio (between minimum and maximum projections) was used to separate inclusions of type C S=0.5 from type D inclusions (Figure 7).

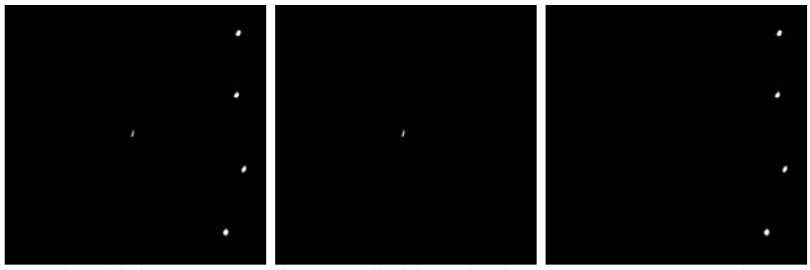

Figure 7 – a) Result of (Figure 6a – Figure 6d). b) Inclusions type C S=0.5. c) Type D inclusions.

6. The union of the images resulting from steps 2 and 4 gives an image with all type B inclusions (see Figure 8a). The union of the images resulting from steps 3 and 5 gives an image with all type C inclusions (Figure 8b).
The final result of the sequence above is shown in Figure 8c, where each type of inclusion is shown in a different color. This classification corresponds exactly to the original types used to build the synthetic image, showing the success of the algorithm. The same sequence was applied to several other images derived from the charts, with equivalent results.

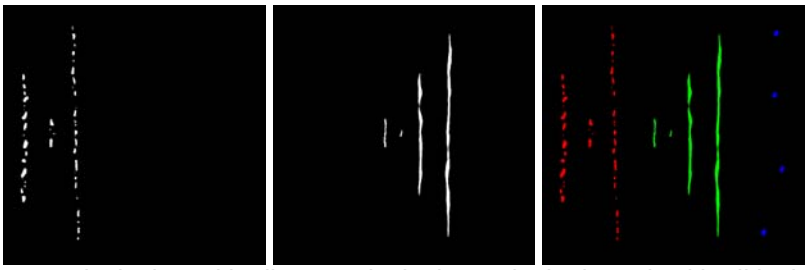

Figure 8 – a) All type B inclusions. b) All type C inclusions. c) Final result with all inclusions of all types and thicknesses. Type B – red. Type C –- green. Type D – blue.

Once the types are identified the thickness and the severity must be measured.

2.2.2 Classification according to thickness

For A and D types the classification by thickness is very simples since it does not depend on stringer formation. The standard just establishes the ranges of thickness for the thin and thick series. Thus, it suffices to measure the projection of each inclusion along an axis orthogonal to RD, which in the present case corresponds to the x projection or feret and compare it to the standard ranges. Figure 9 shows an example for D type inclusions.

Figure 9 – Classification according to thickness. a) Type D inclusions. b) Thin series. c) Thick series.

For B and C types the thickness classification applies to each stringer. However, the thickness depends on the total *length* of thin and thick inclusions in a given stringer. The stringer is defined as thin if the total length of thin inclusions is more than 50% of the total length, and vice-versa. Thus, it was necessary to build stringers, as described before. Figure 10 shows an example for the type B inclusions identified before.

Figure 10 – Identification of stringers – Type B. a) 3 stringers. b) Each inclusion surrounded by its aligned convex hull. c) After horizontal dilation and vertical closing.

Once the stringers are built, a loop scans each stringer to classify each inclusion into the thin or thick series according the standard, and the total length of each series is accumulated separately. That with the largest value defines the thickness of the stringer. Figure 11 shows an example for a B type stringer that is eventually classified as thin.

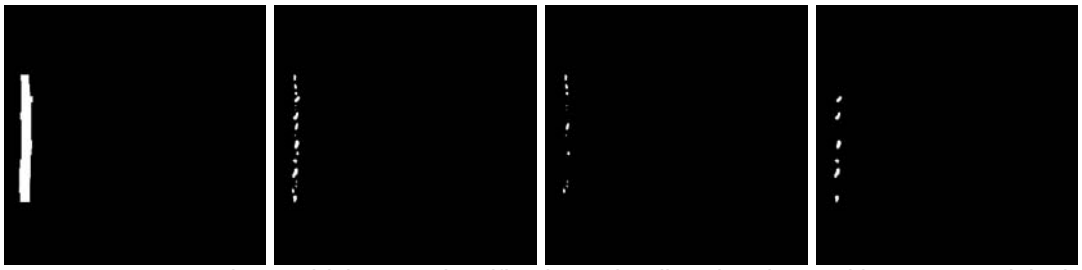

Figure 11 – B type stringer thickness classification. a) Dilated stringer. b) Recovered inclusions pertaining to the stringer. c) Thin inclusions. d) Thick inclusions. The total length of thin inclusions is larger than for thick ones, and the stringer is classified as thin.

Figure 12 shows the final result of thickness classification applied to the result in Figure 8c. Here, the thin or thick series are shown as variations upon the basic color for that type of inclusion. The image is magnified to improve visibility of the result.

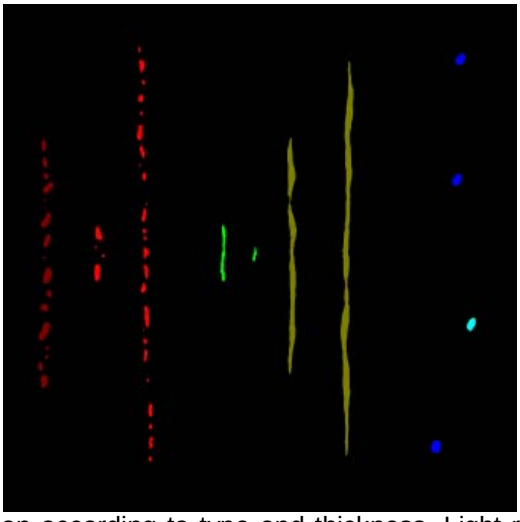

Figure 12 – Final classification according to type and thickness. Light red – type B thin. Dark red – type B thick. Light green – type C thin. Dark green – type C thick. Light blue – Type D thick. Dark blue – Type D thin.

2.2.2 Severity calculation

Once the types and thicknesses of inclusions or stringers have been defined, it is possible to calculate the severity, as described in section 2.1.1. As in the simple cases with separated types and severities, the results for the mixed synthetic images presented small errors.

3 PROCESSING OF REAL IMAGES

The ASTM standard recommends a total area of 160 mm^2 for either manual or automatic classification of inclusions in a given steel sample. This area may be obtained through the combination of fields obtained at any magnification, given that severity measurements are obtained from fields with at least 0.5 mm^2.

These specifications are greatly simplified with the use of a digital microscopy (DM) system. This is the case of the Zeiss Axioplan 2ie motorized optical microscope of the Digital Microscopy Lab of DEMa PUC-Rio. Is has computer controlled x-y specimen scanning, motorized autofocus and objective lens change, coupled to an AxioCam HR digital camera, and controlled the Axiovision software.

The acquired images can be automatically analyzed to detect the presence of inclusions. The software can then move the sample holder back to a field of interest, and acquire higher magnification images that allow a better visualization of the detected inclusions. At higher magnification, however, the field may be too small to adequately represent two relevant characteristics of the microstructure: elongated inclusions and/or long stringers than span more than one field.
This situation can be managed by the DM system through the acquisition of mosaic images composed of adjacent fields, covering an area large enough to show the relevant features completely. This is illustrated in Figure 13 that shows 3 individual fields and a mosaic. It is evident that the individual fields do not reveal correctly the relevant features to be detected. On the other hand, the mosaic image correctly depicts the elongated inclusions on the left and the stringer on the right.

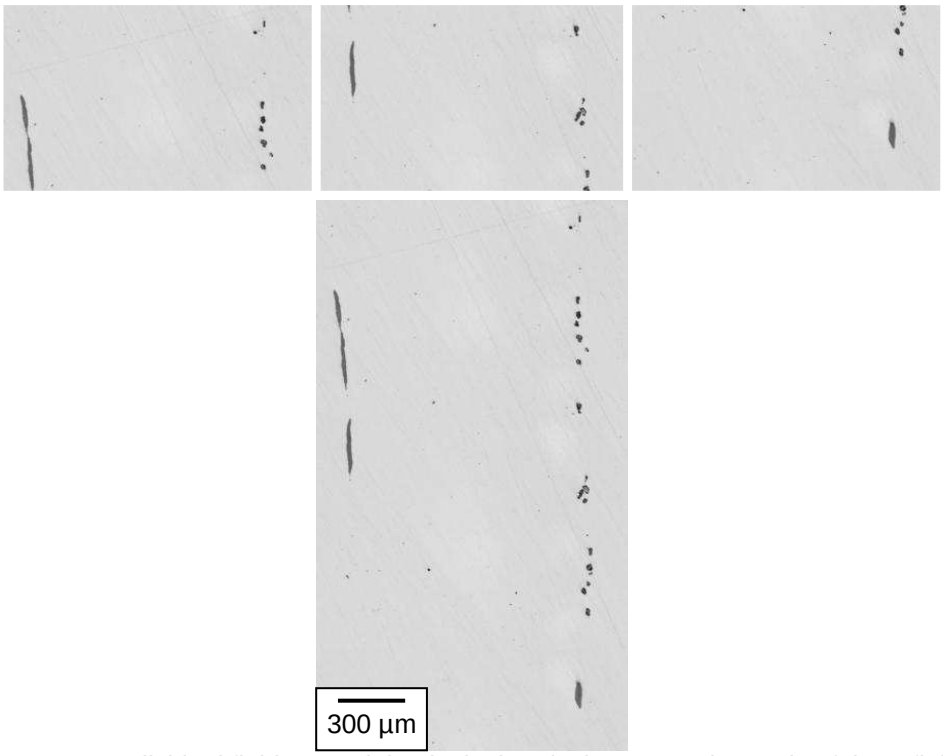

Figure 13 – Individual fields containing inclusions/stringers, and mosaic of the 3 fields.

In principle, the DM system allows acquiring mosaics of any number of fields, potentially covering the recommended analysis surface in a single image. However, for this to be meaningful one must use an objective lens (OL) with enough resolution to reveal the inclusions. On the other hand, the higher the magnification and the better the resolution of the OL, the smaller is the field. Thus the mosaics would be formed by a very large number of fields, and would require such a large image file that image processing would become impractical. Thus, a compromise between resolution, inclusion and stringer size, mosaic file size and inclusion visibility must be reached.
Figure 14a shows a mosaic composed of 3x3 = 9 images acquired with a 50X OL, for a total magnification of ≈ 500X, 0.2 µm/pixel and total area of 0.48 mm^2. This is very close to the minimal field size recommended by the standard, 0.50 mm^2. This mosaic occupies 11.5 Mbytes in grayscale. For the total area of 160 mm^2 a single mosaic would require 3.6 Mbytes, and would be impossible to process. Decreasing the

magnification to 100X (10X OL) would lead to a file of 147 Mbytes, more amenable to processing, but with a correspondingly decreased resolution.

For the example in Figure 14, the steel presented high sulfur content, leading to a large quantity of type A inclusions and a smaller quantity of type D inclusions. For this case, the standard recommendation to separate type A by its lighter gray shade is applicable. However, a few problems appear, and are illustrated in Figure 14b. Many darker type D inclusions appear mixed with type A´s. Moreover, small variations in tonality within the long inclusions may lead to the false identification of type D´s. Measurements of thickness and severity are biased by these problems.

If tonal variations are ignored initially, so that all inclusions are detected together, types A and D can be discriminated by their shape. This is shown in Figure 14c were possible mixed A-D inclusions were ignored, were considered as type A, and classified into the thin (light red) and thick (dark red) series. Separated D inclusions were also detected and classified (blue). Inclusions touching the edge cannot be identified and were eliminated. The severity for each type was then calculated.

The total length for type A thin was 759 µm, or S=2.5, and for type A thick was 326 µm, or S=1.5. This is similar to the visual analysis of an experimented operator that measured S=3 and S=1, for the thin and thick series, respectively. The routine counted 17 thin D inclusions, or S=2. This is much larger than the S=0.5 result given by the same operator. This can be explained by the lower magnification used by the operator (100x), what can impair the detection of smaller inclusions.

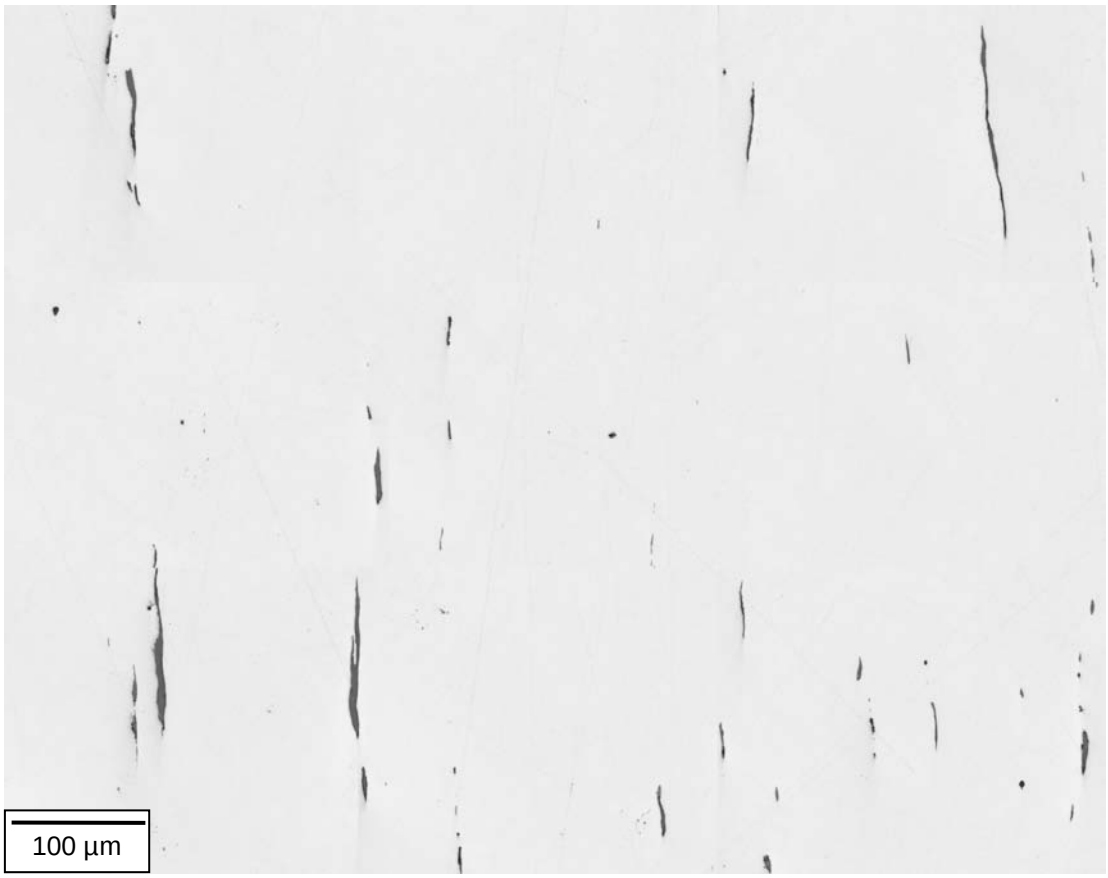

Figure 14 – a) Image mosaic (3x3) of a steel sample with high sulfur content. A large number of type A inclusions is visible, as well as a smaller number of D type oxides.

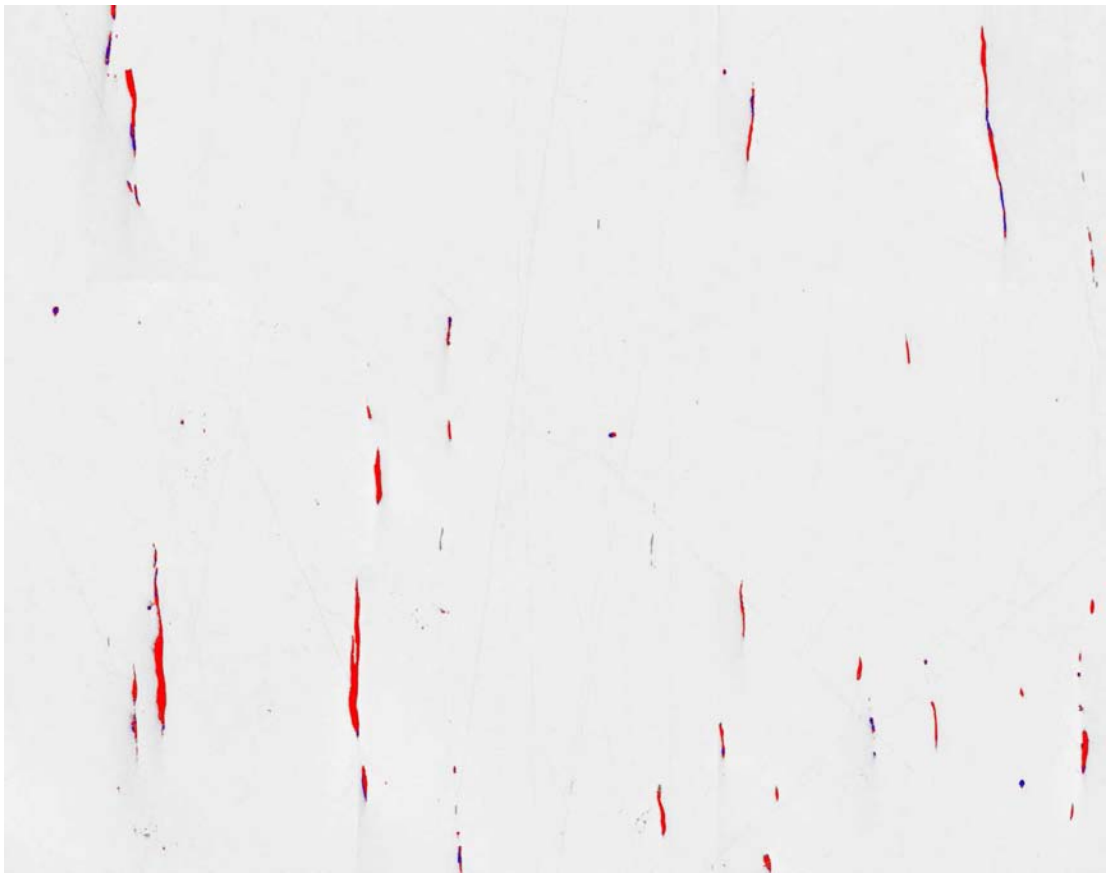

Figure 14 (cont.) b) Result of tonality processing showing A (red) and D (blue) inclusions as well as some mixed inclusions.

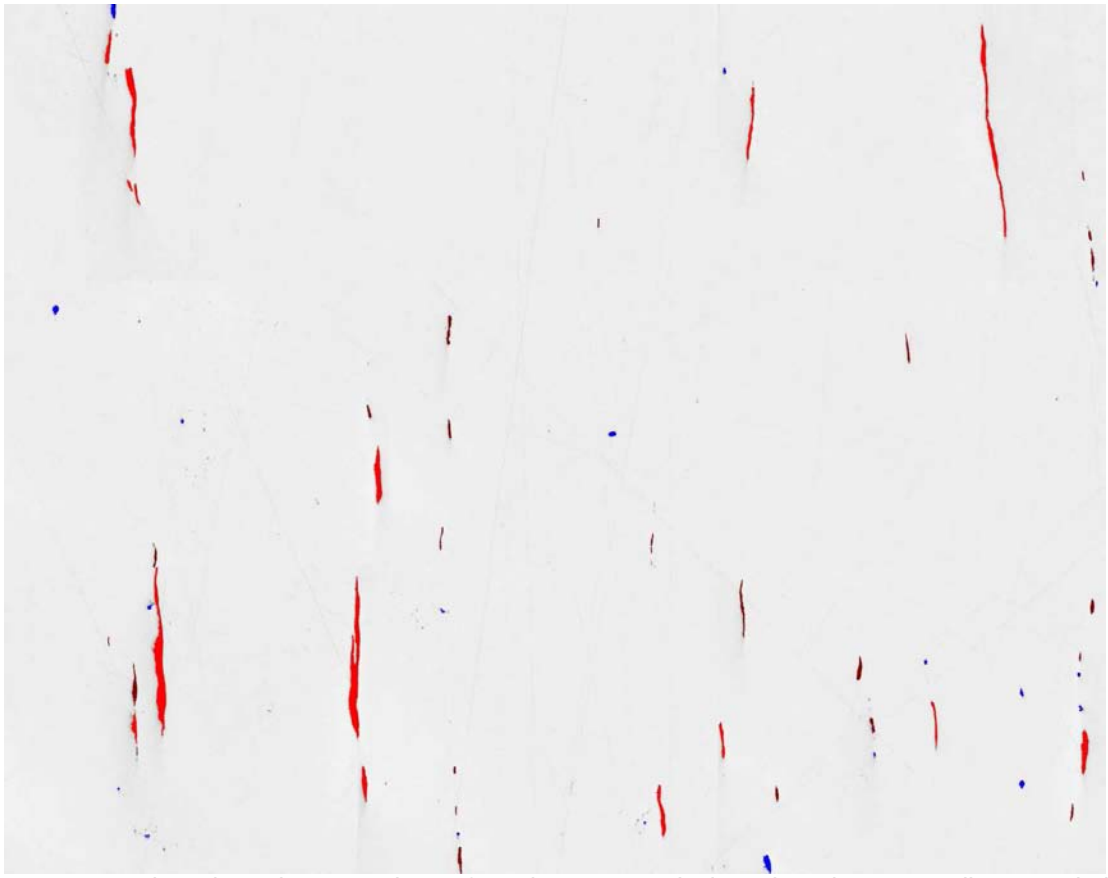

Figure 14 (cont.) c) Result of shape analysis ignoring tonality variations. Possible mixed inclusions are ignored. A thick (red), A thin (dark red) e D thin (blue).

4 CONCLUSIONS

A procedure to automate the classification of inclusions in steels was developed. It employs an image processing and analysis routine that encodes the rules established by the ASTM Standards.

The reference charts from ASTM E-45 were used to develop the algorithm and test its accuracy. In these cases, the developed procedure was able to discriminate inclusions of types B, C, and D, building stringers for types B and C whenever necessary, and measuring thickness and severity for each kind. The accurate measurements of length for inclusions or stringers, for both the thin and thick series, showed the method is reliable.

When applied to real samples the routine also showed good results but a few problems were identified. From a practical point of view, it was difficult to obtain sufficiently “dirty” steels to test the robustness of the routine, especially steels containing types A, B, and C, which are harder to discriminate. So far, the method has not been tested in these situations.

In samples with both A and D types, mixed inclusions posed a different problem. These are included in the standard definitions, but their treatment is much more complicated. Thus, as a simplification, possible mixed inclusions were treated as of single type, what allowed an acceptable discrimination of separated inclusions, as well as the measurement of thickness and severity. A comparison with manual results provided acceptable results. The detailed treatment of mixed inclusions is one of the possible continuations of the present work.

It is also possible to use Scanning Electron Microscopy to discriminate smaller inclusions and combine morphological measurements by IA with chemical analysis by EDX, what would allow a more accurate identification of inclusions, especially of the mixed type.

REFERENCES

1 ASTM E45-97 - Standard Test Methods for Determining the Inclusion Content of Steels – Annual Books of ASTM Standards, Section 3, Volume 03.01, ASTM, West Conshohocken, p163-176,1999.
2 ASTM E1122-96 - Standard Practice for Obtaining JK Inclusion Ratings Using Automatic Image Analysis – Annual Books of ASTM Standards, Section 3, Volume 03.01, ASTM, West Conshohocken, p729-736,1999.
3 RUSS, J. C., Computer Assisted Microscopy, Plenum Press, New York, 1992.
4 PACIORNIK, S.; MAURICIO, M. H. P., Digital Imaging in ASM Handbook – Metallography and Microstructures, ed. VANDER VOORT, G. F., Vol. 9, ASM International, Materials Park, p368-402, 2004.